HEAT TRANSFER IN THE TIP REGION OF A ROTOR BLADE SIMULATOR*

M.K. Chyu, H.K. Moon and D.E. Metzger
Mechanical and Aerospace Engineering Department
Arizona State University
Tempe, AZ 85287

INTRODUCTION

In gas turbines, the blades of axial turbine stages rotate in close proximity to a stationary peripheral wall (sometimes termed an outer ring or stationary shroud). Differential expansion of the turbine wheel, blades, and the shroud causes variations in the size of the clearance gap between blade tip and stationary shroud. The necessity to tolerate this differential thermal expansion dictates that the clearance gap cannot be eliminated altogether, despite accurate engine machining [1].

Pressure differences between the pressure and suction sides of a blade drives a flow through the clearance gap. This flow, often referred as the "tip leakage" flow, is detrimental to engine performance. The primary detrimental effect of tip leakage flow is the reduction of turbine stage efficiency, and a second important effect concerns the convective heat transfer associated with the flow. The surface area at the blade tip in contact with the hot working gas represents an additional thermal loading on the blade which, together with heat transfer to the suction and pressure side surface area, must be removed by the blade internal cooling flows [2].

Very limited information on turbine tip heat transfer and fluid flow has been reported to date [3-6], and almost all of the published work dealing with clearance gap flows involves consideration only of plain flat blade tips. However, a strategy commonly employed to reduce tip flow and heat transfer is to groove a single rectangular cavity chordwise along the blade tip. The groove acts like the cell of a labyrinth seal to increase the pressure drop and thus reduce the flow for a given pressure differential across the tip. The reduction of the flow will also act to reduce heat transfer. A schematic diagram representing the geometry of a grooved blade tip, viewed from a coordinate system fixed relative to the blade, is shown in Fig. 1. As seen in the figure, the outer shroud can be considered moving in the general direction from the suction side to the pressure side, with relative velocity equal to U_w. The leakage flow, its mean value denoted by $\bar{U}$, is driven by the pressure difference between two sides of the blade and flows in the direction opposite to the shroud motion.

*Work done under NASA Grant NAG 3-623

With this general configuration in mind, the grooved tip problem can be categorized as fluid flow and heat transfer over a shrouded rectangular cavity.

Both fluid flow and heat transfer over unshrouded, rectangular cavities have been the subjects of extensive investigation for many years [7]. The flow field over a cavity is characterized by flow separation and shear layer reattachment resulting in complex flow patterns with substantial effects on the friction drag and heat transfer. Most studies have relied on flow visualization techniques and/or heat and mass transfer data to obtain momentum and heat transfer information in cavity flow [8-10]. In all cases, the cavity problems studied have been considered as a flow system in which the cavity is open to a usually well-specified approaching flow over an otherwise smooth and stationary surface. The approaching flow may be a wall boundary layer for external flow or a well developed channel flow.

The grooved tip differs from the aforementioned unshrouded situation by virtue of the confined nature of the geometry as well as by the proximity of moving shroud. The degree of similarity between the heat transfer characteristics of the grooved tip and those of previous cavity studies has been unclear until recently. Metzger and Bunker [11], using a time-dependent paint coating technique, studied the heat transfer for flow through a confined narrow slot-type channel where one of the bounding walls contains a rectangular cavity. The effect of shroud motion is not included in this study. Details of heat transfer on the cavity surfaces are found to be largely dependent on the size of gap clearance and the cavity aspect ratio. A semi-empirical study by Mayle and Metzger [6], using a plain tip geometry, has argued that the heat transfer from the blade tip is essentially unaffected by the relative motion between blade and shroud. This speculation, however, has not been justified for the grooved tip situation. To gain further understanding of the convective heat transfer in cavities with various degrees of relative shroud motion is the primary objective of this study.

In the present work, experimental results concerned with the local heat transfer characteristics on all surfaces of shrouded, rectangular cavities are reported. The varying parameters include the cavity depth-to-width ratio, D/W, gap clearance-to-cavity width ratio, C/W, relative shroud moving speed, $U_w/\bar{U}$, Reynolds number, $Re = \bar{U}C/\nu$, and relative orientation between the leakage flow direction and shroud movement. Due to the problems associated with imperfect thermal insulation and temperature depression, local studies using direct heat transfer measurement are known to be difficult to perform and could induce significant error. The naphthalene ($C_{10}H_8$) sublimation mass transfer technique is instead employed herein facilitating better control of the experiment. The mass transfer results can be transformed into their counterparts in heat transfer by invoking an analogy between those two transfer processes. More detailed description of the analogy can be found in [12]. A brief discussion of the mass transfer system used in this study is given as follows.

SUBLIMING MASS TRANSFER SYSTEM

The mass transfer coefficient h_m is given by

$$h_m = \frac{\dot{m}}{\rho_{v,w} - \rho_{\infty}} \tag{1}$$

where, $\dot{m}$ is the mass transfer flux of naphthalene from a surface, $\rho_{v,w}$ is the vapor concentration of naphthalene at the surface, and ρ_{∞} is the vapor mass concentration at the inlet of gap passage. In the present study, ρ_{∞} is zero and Eq. (1) becomes

$$h_m = \frac{\dot{m}}{\rho_{v,w}} \tag{2}$$

In addition, as the mass transfer system is essentially maintained isothermal, the naphthalene vapor pressure and vapor concentration at the surface are constant. This corresponds to a constant wall temperature boundary condition in a heat transfer study.

Local mass transfer from a naphthalene surface can be evaluated from the change in naphthalene thickness. The change of thickness due to sublimation is given by

$$dy = \frac{\dot{m} \cdot dt}{\rho_s} \tag{3}$$

where ρ_s is the density of solid naphthalene ($\simeq 1.143$ gm/cm^3), and dy and dt represent the change in naphthalene thickness and the differential time duration, respectively. Note that dy and $\dot{m}$ are functions of the local coordinate of the subliming surface. Combining Eqs. (2) and (3), and integrating over the test duration yield the time-averaged, local mass transfer coefficient

$$h_m = \frac{\rho_s \cdot \Delta y}{\rho_{v,w} \cdot \Delta t} \tag{4}$$

The mass transfer Stanton number is defined by

$$St = \frac{h_m}{\bar{U}} \tag{5}$$

As it is often the case that the wall temperature varies slightly during test run, $\rho_{v,w}$ can be represented by the time-averaged naphthalene concentration at the surface. This is obtained from numerical integration of the concentration determined at the measured surface temperature. A correlation proposed by Ambrose et al. [13] is used to determine naphthalene vapor pressure, from this, $\rho_{v,w}$ is evaluated using the ideal gas law and the naphthalene surface temperature.

EXPERIMENTAL APPARATUS AND PROCEDURE

Fig. 2 displays schematic view of the test section. The entire construction is made of aluminum tooling plates. The shaded area in the figure, representing a cavity-like grooved tip, is the mass transfer active surface cast with a thin layer of naphthalene, approximately 2 mm in thickness. The cavity width, W, is maintained constant at 3.2 cm (1.25 inch) throughout the entire study. The desired values of C/W and D/W can be obtained accordingly, by fixing a pair of adjustable screws. A 1.6 cm width surface is extended both upstream and downstream of the cavity, forming the upstream gap and downstream gap, respectively. The cavity span normal to the streamwise direction is measured at 15.3 cm (6.0 inch) which is approximately four times of the streamwise width, W. Under this condition, although possible three-dimensional phenomena are expected, preliminary tests have shown that the mass transfer characteristics are very much two dimensional across at least 80% of the span. The moving shroud is modeled by a flat, seamless, Neoprene belt driven by a speed-adjustable, 3/4 HP. D.C. motor. The test assembly can be rotated in different orientation relative to the belt moving direction.

During a test run, the laboratory compressed air supply is first introduced to a plenum adjacent to the test cavity, then flows over the cavity, and subsequently discharges to the surrounding atmosphere. The entire test assembly including plenum and cavity is placed above and contacts the moving belt, with the cavity opening facing downward. Between the test assembly and the moving belt, there are several teflon pads mounted on the contacting surface of the test assembly to reduce dynamic friction and to prevent air leakage. An additional teflon plate is placed underneath and against the belt which effectively eliminates belt vibration as it moves over the test section. Preliminary tests at full anticipated belt speeds indicate that this design is very effective.

One of the most challenging aspects of the subliming mass transfer experiment is the surface profile measurement on the naphthalene surface. Mass transfer at a certain location is inferred from the change in naphthalene thickness at that location. In order to obtain the distribution of local mass transfer coefficient in the region of interest, the surface contour must be measured before and after each test run. Therefore, successful execution of local measurements in subliming mass transfer is critically dependent on precise positioning and accurate thickness change readings. In addition, to avoid errors caused by the extraneous naphthalene sublimation and human fatigue during a lengthy measurement requires rapid data acquisition. A computer-controlled, automated data acquisition system has been designed and used to fulfill all of these requirements. A block diagram giving a schematic view of the entire system is shown in Fig. 3. It consists of a depth gauge along with a signal conditioner, a digital multimeter, two-stepper-motor driven positioners, a motor controller, and a Zenith 150 microcomputer (IBM-PC compatible) as the measurement process controller. The Zenith microcomputer is also used for data storage and reduction. Details of the measurement system have been described in [14, 15].

RESULTS AND DISCUSSION

Most of the mass transfer results in this study are presented in form of Stanton number, St, as discussed in the previous section. For all the test runs, the uncertainty in the local St is estimated to be 5%, and the repeatability is considerably better than this value. Prior to the actual tests for grooved-tip geometries, mass transfer from a flat surface in the absence of cavity has been measured, and the results agree very well with those of heat transfer in the developing region for turbulent pipe flow with a sharp-angle entrance [16]. This validates the present experimental system and provides confidence in data accuracy.

A sample of results describing the local Stanton number distribution on the cavity floor and the surfaces of upstream and downstream of the cavity is shown in Fig. 4. The figure consists of four sub-figures, 4(a) to 4(d), representing $Re = \bar{U}C/\nu = 2.0 \times 10^4$, $C/W = 0.14$, and $D/W = 0.1$, 0.5, 1.0, and 1.5, $U_w/\bar{U} = 0.0$ and 0.46. It is noted in Fig. 4 that very non-uniform St distributions exist for all the cases tested. On the surface upstream of the cavity (i.e. the upstream gap), St increases with streamwise location, reaches a local maximum near the mid-point of the surface, and then decreases toward downstream. The characteristic of this St distribution is virtually identical to that of heat transfer near a channel entrance preceded by a sudden contraction. Typical value of the maximum St is approximately twice as that for the fully developed channel flow having the same Reynolds number.

Mass transfer characteristics on the surface downstream of the cavity (i.e. downstream gap) are similar to that of a newly developing boundary layer with zero angle of incidence. In contrast to the upstream gap, the highest St occurs near the leading edge of the surface, and the St decreases along the streamwise direction. However, it is speculated that a second local maximum St may exist somewhere downstream of the leading edge provided that the gap size is sufficiently large; a vortex region is expected to exist in the upstream portion of this surface. This second local maximum St has been reported in the literature for cavity flow without shroud presence [10].

Values of St on the cavity floor are in general smaller than that on surfaces upstream and downstream of the cavity. In addition, as shown in Fig. 4, the nature of the cavity-floor St distribution depends strongly on the cavity geometry, namely the cavity aspect ratio, D/W. For shallow cavities, say $D/W = 0.1$, the shear layer separated from the upper corner of the cavity upstream wall should have reattached the cavity floor. In the region near the reattachment point, generally accompanied with higher turbulence mixing, mass transfer coefficient reaches a local maximum. This effect is clearly observed in Fig. 4(a). For $D/W = 0.5$, according to a flow visualization study on unshrouded cavities [9], the entire cavity will be largely filled with a recirculating vortex resulting in a streamwise, monotonically increasing trend of mass transfer on the cavity floor, as shown in Fig. 4(b). For even deeper cavities,

D/W = 1.0 and 1.5, the values of cavity-floor St become smaller, and peculiar mass transfer characteristics exist, with more than one local maximum St being observed in Figs. 4(c) and (d). This is speculated to be attributable to the additional and strong degree of secondary-flow interactions near the cavity bottom.

For all the cases present in Fig. 4, the general trend of influence of relative shroud movement on the mass transfer from a grooved tip is found to be quite consistent. At each corresponding streamwise location, the mass transfer St on the surfaces of downstream gap and cavity floor are generally higher for $U_w/\bar{U}$ = 0.46 than that for stationary shroud situation (i.e. $U_w/\bar{U}$ = 0); while the reversed effect is observed on the surface of upstream gap. This is understandable that the shroud motion introduces more naphthalene-free air into the mainstream in the downstream portion of the test section, thus the bulk air flow in this region is less naphthalene-enriched than that without shroud motion. This in turn enhances the mass transfer. Opposite effect is expected for the upstream portion, resulting in a lower mass transfer driving potential. However, the difference in St affected by the different values of $U_w/\bar{U}$ is overall insignificant and, for majority of the data, the differences are in fact within the experimental uncertainty. The speculation raised in Ref. [6] that the relative shroud motion has a very minor effect on the flat blade-tip heat transfer may also be applied to the heat transfer to a grooved tip, at least for the present study range.

Mass transfer measurements are also made on cavity side walls, and Figs. 5 and 6 show typical results for the intermediate cases D/W = 0.25 and 1.0. The mass transfer from the cavity upstream wall (downstream-facing wall) is dominated by the vortex attached behind the wall and has the same order of magnitude of St as that on the upstream portion of cavity floor, which generally has low mass transfer rates. On the other hand, the fundamental mode of mass transfer mechanism for the cavity downstream wall (upstream-facing wall) is the impingement of the separated shear layer on the wall, in particular on the upper portion. As a result, the mass transfer coefficient is generally high near the top of the downstream wall. The influence of relative shroud movement on the mass transfer from the two side walls is found to be insignificant, the same finding shown in Fig. 4. However, the influence seems to be stronger for deeper cavity (D/W = 1.0) than for the shallower one (D/W = 0.25), and, as shown in Fig. 6, it affects oppositely on the mass transfer between upstream and downstream walls.

Fig. 7 shows the area-averaged mass transfer coefficient and the overall mass transfer rate for all the cases presented in Fig. 4. The left scale in Fig. 7 represents the Stanton number averaged over the entire mass transfer active region, $\overline{St}$; while the right scale gives the value of $\dot{M}_t/\rho_{v,w}$ normalized by the corresponding value for the case D/W = 1.0, where $\dot{M}_t$ is the time-averaged mass transfer rate over the entire mass transfer surface. As expected, the shroud motion has little influence on both results, with a less than 10% maximum variation caused by the difference in shroud movement. According to Fig. 7, $\overline{St}$ decreases with an increase in the value of D/W; however,

the value of normalized overall mass transfer rate remains almost constant for $D/W \leq 0.5$ and then increases for higher D/W values. This implies that, despite the lower mass transfer coefficient, the deeper cavities experience higher overall mass transfer rate than the shallower ones, due mainly to the additional mass transfer area present in the cavity side walls. If the heat transfer with tip leakage flow is of concern, it may be undesirable to groove a blade tip having a cavity aspect ratio, D/W, higher than 0.5. This result agrees favorably with the conclusion from Ref. [11] by Metzger and Bunker.

Another important parameter affecting the tip heat transfer is the size of gap clearance, namely C/W. Fig. 8 shows the typical results for cavities with $D/W = 1.0$, $Re = 2.0 \times 10^4$, and $U_w/\bar{U} = 0$. The general trend is that the larger the value of C/W, the higher the mass transfer coefficient. In addition to change in the magnitude of local St, the general characteristics of St distribution over the surfaces of upstream and downstream gap vary with different values of C/W. This variation may be understood by consideration of flow pattern in the gap, which, to a certain extent, is affected by the nature of sudden contraction as the fluids flow into the gap. Moreover, according to a recent study by Chyu et al. [17], the larger gap clearance permits the separated shear layer to grow thicker inducing higher turbulence level in the gap mainstream. The mass transfer on the downstream gap surface as well as on the cavity downstream wall are thus influenced by the characteristics of shear layer. In view of the results shown in Fig. 8, a recirculating vortex may exist in the downstream gap for $C/W \geq 0.2$., as a local minimum of St observed in the mid-portion of the surface.

Fig. 9 shows the Reynolds number effect on the tip mass transfer. While fixing the $D/W = 1.0$ and $C/W = 0.14$, the Reynolds number, defined as $Re = \bar{U}C/\nu$, varies from 0.38×10^4 to 3.6×10^4 by controlling the air flow from the laboratory compressor. Since the size of clearance is physically the same in these cases, the only variable in fact is the gap mean velocity. As shown in Fig. 9, within the present test range, the local St generally decreases with an increase of Re. However, the trend is attenuated and even reversed when $Re \geq 3.6 \times 10^4$. This peculiar tendency can be explained at least by consideration of the compressibility effect. For $Re = 3.6 \times 10^4$, Mach number in the gap is approximately equal to 0.4, and it may be inappropriate to consider the flow incompressible, and the mass transfer increases as the compressibility effect dominates.

The actual turbine blade involves curved surfaces, and at a certain location on blade tip, the relative direction between the leakage flow and the shroud movement may not be exactly opposite (180°). Complex secondary flow possibly with helix motions is expected in the tip groove under this condition. As a preliminary investigation of this phenomena, an attempt has been made to study this effect on tip leakage heat transfer by varying the relative orientation between the moving belt and the mass transfer test assembly. The angle varies from 180° to 112°. Fig. 10 displays the contours of constant Stanton number on the cavity floor with a 135° angle of mis-alignment,

C/W = 0.14, D/W = 1.0, $U_w/\bar{U}$ = 0.46 and Re = 2.0 x 10^4. To be noted is the fact that, except for the angle difference, the test condition and geometry are identical to that of results shown in Fig. 4(c). Comparing these two cases, the local mass transfer characteristics apparently are affected by the angle magnitude. However, the overall values of average Stanton number and mass transfer rate are virtually uninfluenced, as shown in Fig. 11.

Attention is now turned to the correlation between the area-averaged mass transfer and the affecting parameters as previously discussed. Using the power regression fit, $\overline{St}$ is found to vary with -0.24 power of D/W, and the power index becomes -0.28 if the area-averaged St over the cavity floor is only of concern. The latter is in good agreement with results from previous studies; -0.22 in Ref. [11] and -0.27 in Ref. [9]. It should be noted that, in Ref. [9], only the cavity floor was heated and the cavity side walls were kept adiabatic, whereas the present mass transfer system is equivalent to the situation with the entire cavity surface maintained at an isothermal wall condition. As for the gap clearance dependency, $\overline{St}$ groups well with C/W to a 0.32 power indicating that a greater influence on tip heat transfer than does the cavity aspect ratio, D/W. The same conclusion has also been found in Ref. [11]. The influence of Reynolds number on the entire tip mass (heat) transfer can be expressed as $\overline{St}$ proportional to $Re^{-0.36}$. In Ref. [9], for unshrouded cavities, the Stanton number averaged over the cavity floor is found to vary as the -0.5 power of Reynolds number. The difference may be attributed to the difference in the nature of cavity geometry, the boundary condition and the testing range of Reynolds number.

CONCLUDING REMARKS

The present study of heat transfer in the tip region of a rotor blade simulator is now in its second-year stage. The naphthalene mass transfer technique with the high-precision surface measurement system has demonstrated itself as a viable method to study the local transfer information in great detail. Parameters which influence the heat transfer in a grooved tip region have been identified, with their effects being investigated extensively. Further studies emphasizing actual blade airfoil shape may be desirable.

REFERENCES

1. Hennecke, D.K., "Heat Transfer Problems in Aero-Engines," Heat and Mass Transfer in Rotating Machinery, D.E. Metzger and N.H. Afgan, eds. Hemisphere, Washington, D.C., 1984, pp. 353-379.

2. Metzger, D.E. and Mayle, R.E., "Heat Transfer Gas Turbine Engines," Mech. Eng., 105, No. 6, June 1983, pp. 44-52.

3. Lakshminarayana. B., "Methods for Predicting the Tip Clearance Effects in Axial Flow Turbomachinery," J. Basic Eng, Trans. ASME, 92, 1970, pp. 467-482

4. Booth, T.C., Dodge, P.R. and Hepworth, H.K., "Rotor-Tip Leakage: Part I - Basic Methodology," J. Eng. for Power, Trans. ASME, 104, 1982, pp. 154-161.

5 Wadia, A.R. and Booth, T.C., "Rotor-Tip Leakage: Part II - Design Optimization Through Viscous Analysis and Experiment, J. Eng. for Power, Trans. ASME, 104, 1982, PP. 162-169.

6. Mayle, R.E. and Metzger, D.E., "Heat Transfer at the Tip of an Unshrouded Turbine Blade," 7th International Heat Transfer Conference, Munich, 3, 1982, pp. 87-92.

7. Aung, W., "Separated Force Convection," Keynote Paper, ASME/JSME Thermal Eng. Conf., Honolulu, March 20-24, 1983.

8. Haugen, R.L. and Dhanak, A.M., "Heat Transfer in Turbulent Boundary-Layer Separation over a Surface Cavity," J. Heat Transfer, 89, 1967, pp.335-340.

9. Yamamoto, H., Seki, N. and Fukusako, S., "Forced Convection Heat Transfer on Heated Bottom Surface of a Cavity," J. Heat Transfer, 101, 1979, pp. 475-479.

10. Chyu, M.K. and Goldstein, R.J., "Local Mass Transfer in Rectangular Cavities with Separated Turbulent Flow," Proceedings of 8th Int. Heat Transfer Conf., 3, 1986, pp. 1065-1070.

11. Metzger, D.E. and Bunker, R.S., "Cavity Heat Transfer on a Grooved Wall in a Narrow Flow Channel," ASME Paper 85-HT-57, 1985.

12. Eckert, E.R.G., "Analogies to Heat Transfer Processes," Measurements in Heat Transfer, ed. by Eckert, E.R.G. and Goldstein, R.J., Hemisphere Publication, Washington D.C., 1976.

13. Ambrose, D., Lawenson, I.J. and Sprake, C.H.S., "The Vapor Pressure of Naphthalene," J. Chem. Thermo., 7, 1975, pp. 1173-1176.

14. Goldstein, R.J., Chyu, M.K. and Hain, R.C., "Measurement of Local Mass Transfer on a Surface in the Region of the Base of a Protruding Cylinder with a Computer-Controlled Data Acquisition System," Int. J. Heat and Mass Transfer, 28, 1985, pp. 977-985.

15. Metzger, D.E., Chyu, M.K. and Moon, H.K., "Heat Transfer in the Tip Region of a Rotor Blade Simulator," NASA-Lewis 4th Host Workshop, Cleveland, Oct. 22-23, 1985.

16. Boetler, L.M.K., Young, G. and Iverson, H.W., "An Investigation of Aircraft Heaters XXVII - Distribution of Heat Transfer Rate in the Entrance Region of a Tube," NACA TN 1451, 1948.

17. Chyu, M.K., Metzger, D.E. and Hwan, C.L., "Heat Transfer in Shrouded Rectangular Cavities," AIAA/ASME Thermophysical and Heat Transfer Conference, June 2-4, 1986, Boston.

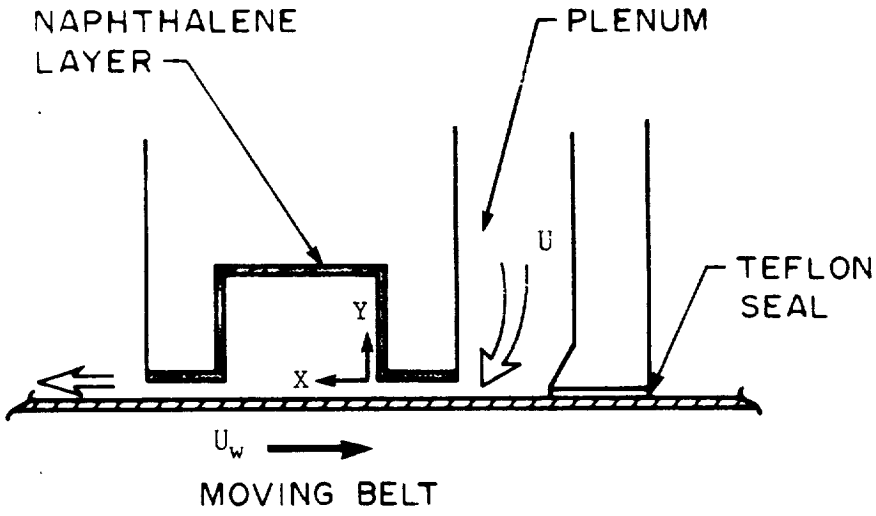

Fig. 1 Schematic View of Test Section

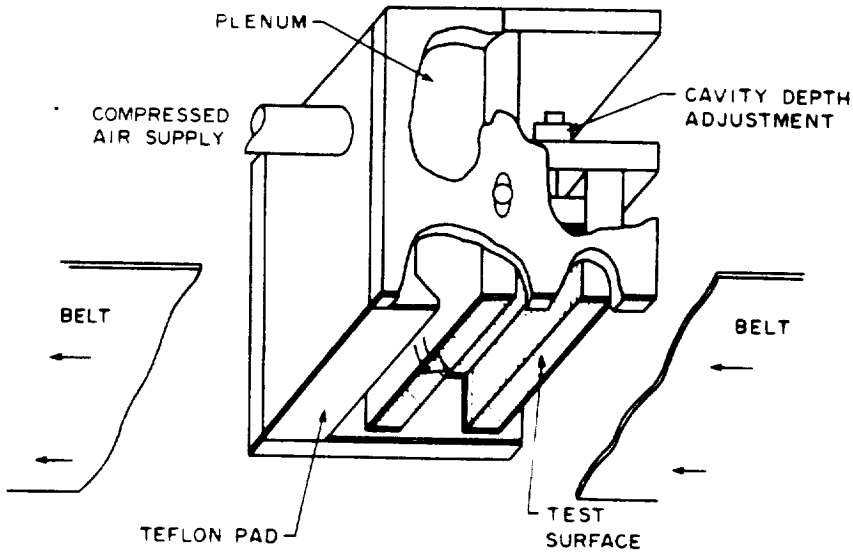

Fig. 2 Schematic View of Test Assembly

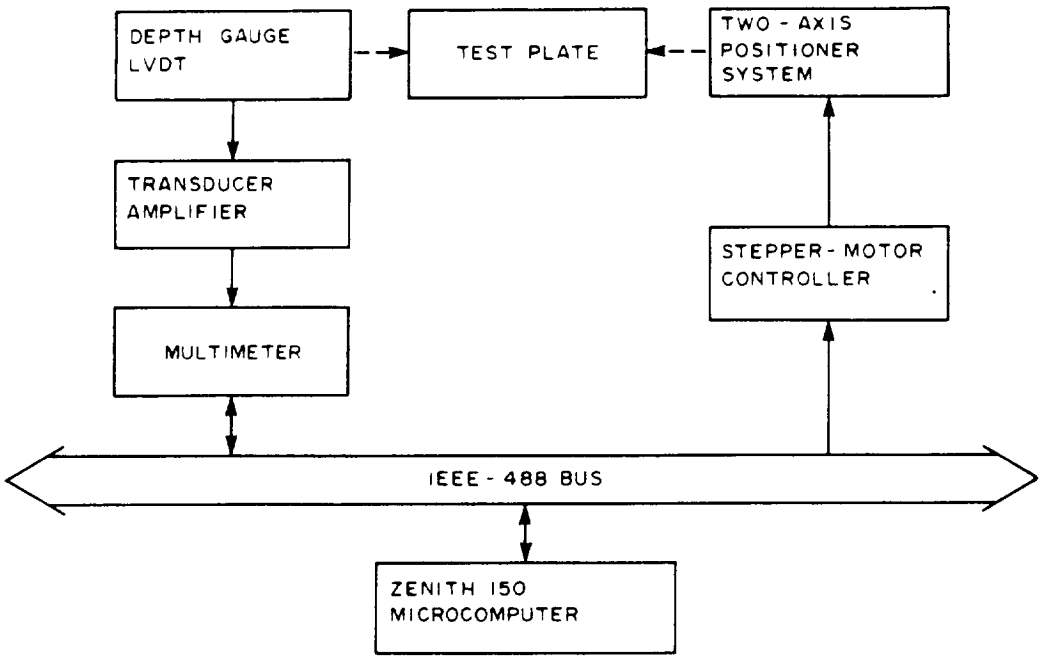

Fig. 3 Local Mass Transfer Surface Measurement System

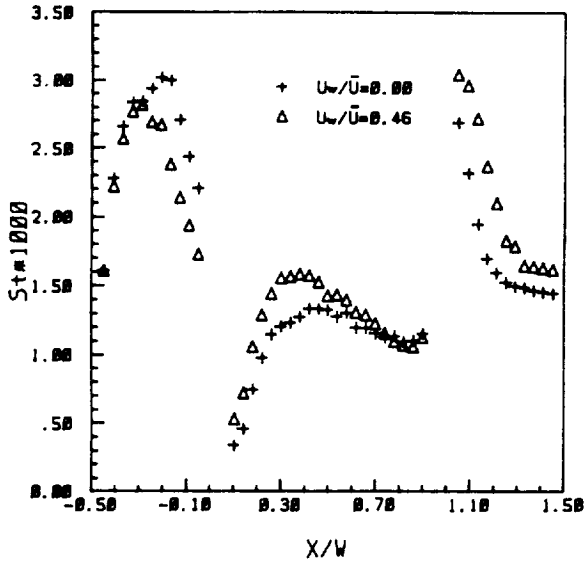

(a) D/W = 0.1

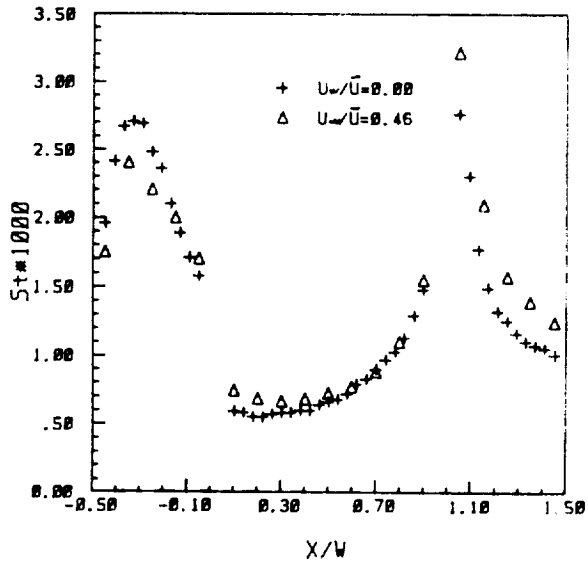

(b) D/W = 0.5

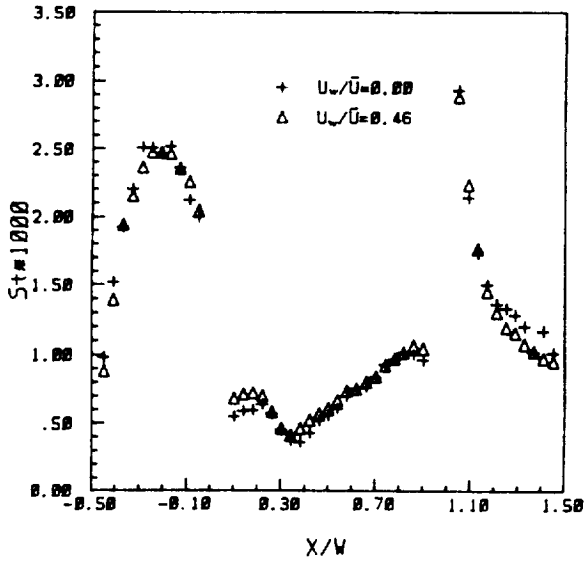

(c) D/W = 1.0

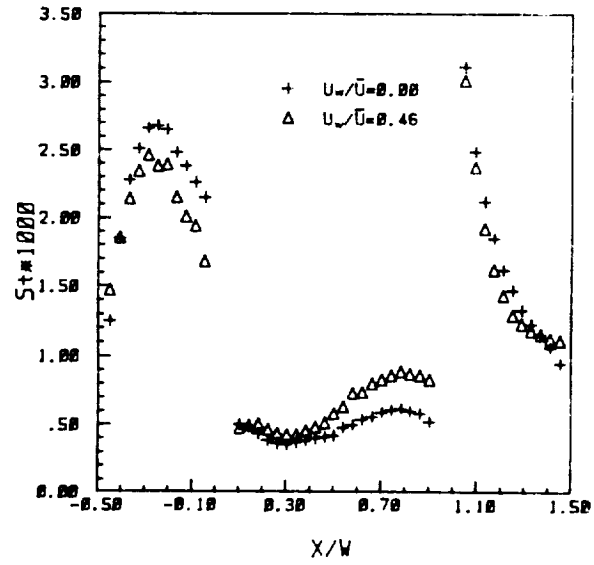

(d) D/W = 1.5

Fig. 4 Local St Distribution in Streamwise Direction; C/W = 0.14, Re = 2.0 x 10^4;

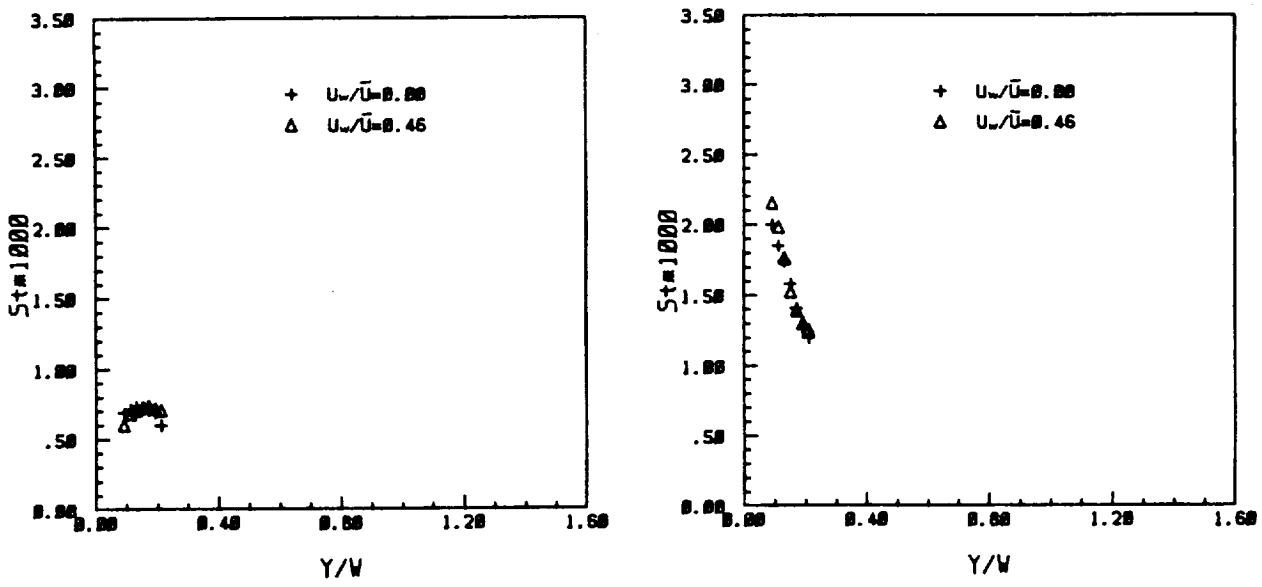

(a) Upstream Wall (b) Downstream Wall

Fig. 5 Local St Distribution on Cavity Side Walls;
C/W = 0.14, D/W = 0.25, Re = 2.0 x 10^4

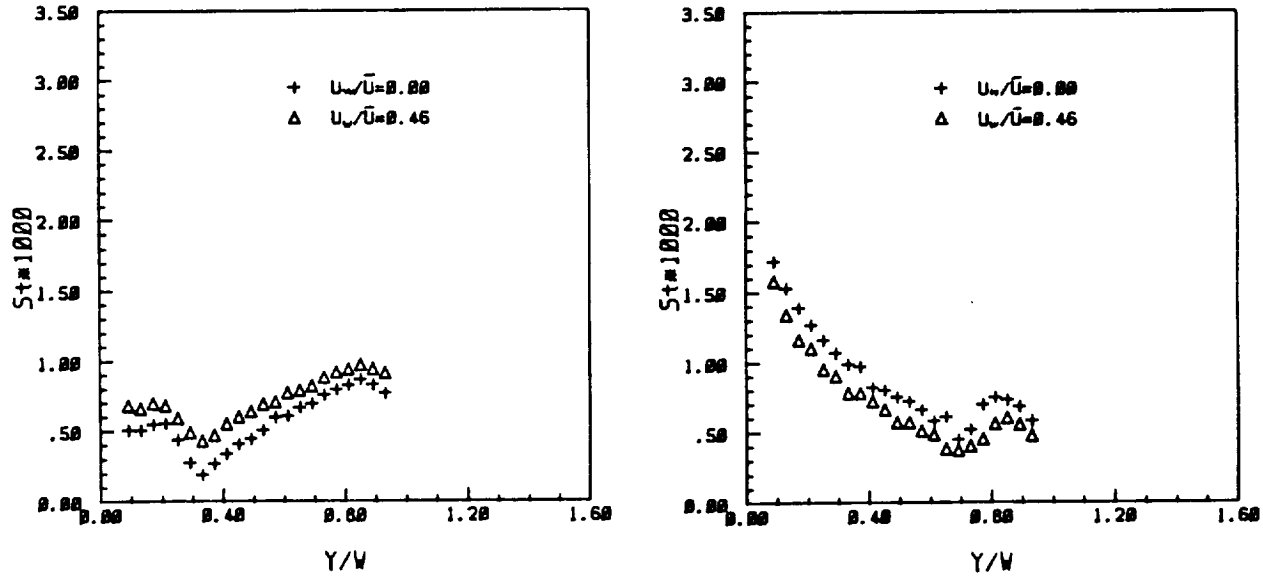

(a) Upstream Wall (b) Downstream Wall

Fig. 6 Local St Distribution on Cavity Side Walls;
C/W = 0.14, D/W = 1.0, Re = 2.0 x 10^4

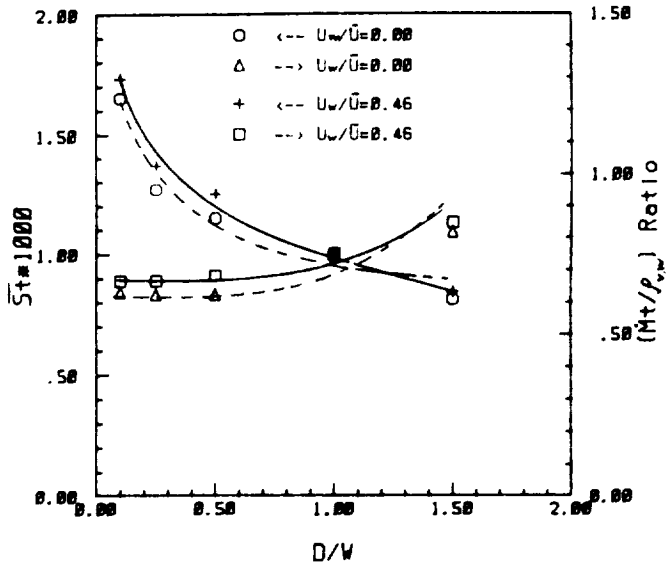

Fig. 7 Area-Averaged Mass Transfer;
C/W = 0.14, Re = 2.0 x 10^4

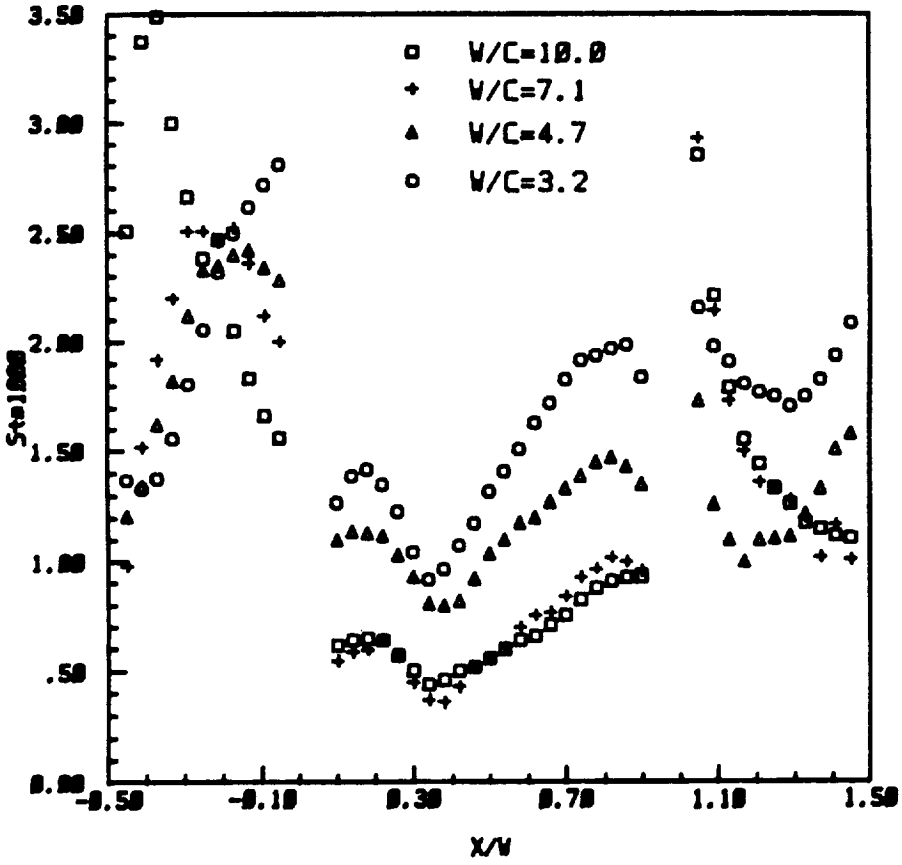

Fig. 8 Gap Clearance Effect on Mass Transfer;
D/W = 1.0, Re = 2.0 x 10^4, $U_w/\bar{U}$ = 0.0

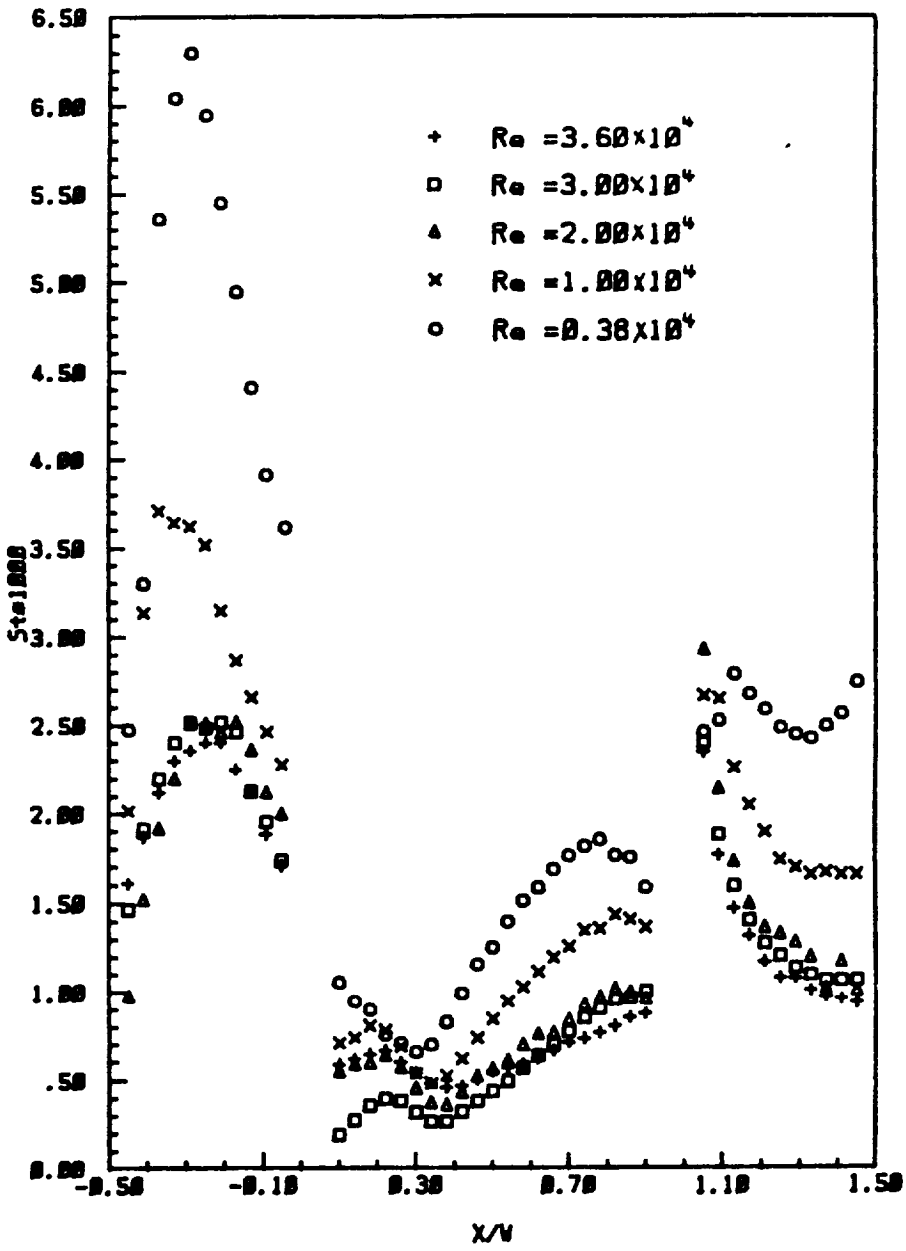

Fig. 9 Reynolds Number Effect on Mass Transfer; C/W = 0.14, D/W = 1.0, $U_w/\bar{U}$ = 0.0

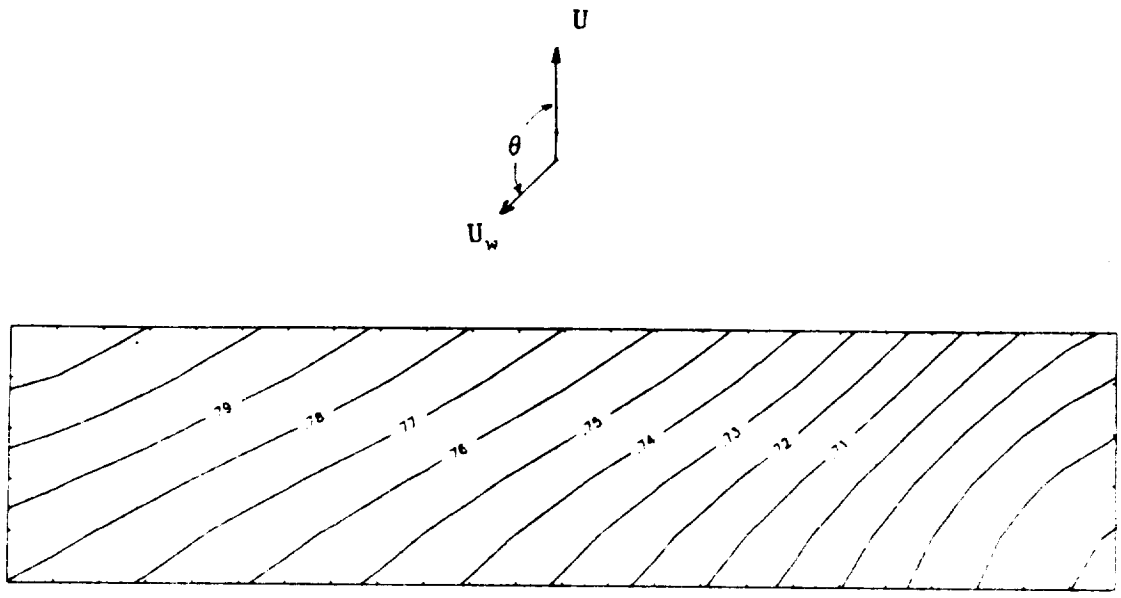

Fig. 10 Stanton Number (St x 10^3) Distribution on Cavity Floor; C/W = 0.14, D/W = 1.0, Re = 2.0 x 10^4, $U_w/\bar{U}$ = 0.46, Θ = 135°

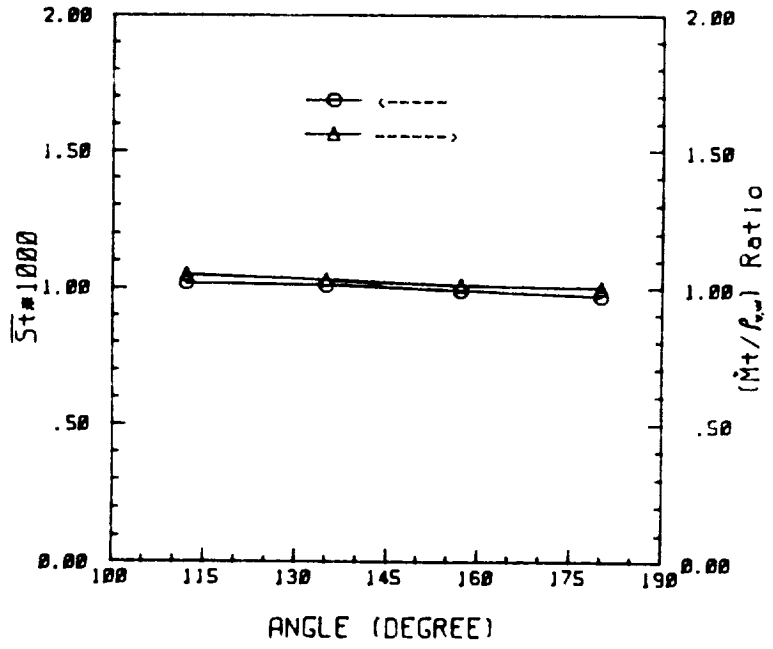

Fig. 11 Shroud-to-Cavity Orientation Effect on Mass Transfer; C/W = 0.14, D/W = 1.0, Re = 2.0 x 10^4, $U_w/\bar{U}$ = 0.46